

Asymmetry Analysis of Bilateral Shapes

Kanti V. Mardia, Xiangyu Wu, John T. Kent, Colin R. Goodall,
Balvinder S. Khambay

Abstract

Many biological objects possess bilateral symmetry about a midline or mid-plane, up to a “noise” term. This paper uses landmark-based methods to measure departures from bilateral symmetry, especially for the two-group problem where one group is more asymmetric than the other. In this paper, we formulate our work in the framework of size-and-shape analysis including registration via rigid body motion. Our starting point is a vector of elementary asymmetry features defined at the individual landmark coordinates for each object. We introduce two approaches for testing. In the first, the elementary features are combined into a scalar composite asymmetry measure for each object. Then standard univariate tests can be used to compare the two groups. In the second approach, a univariate test statistic is constructed for each elementary feature. The maximum of these statistics lead to an overall test statistic to compare the two groups and we then provide a technique to extract the important features from the landmark data. Our methodology is illustrated on a pre-registered smile dataset collected to assess the success of cleft lip surgery on human subjects. The asymmetry in a group of cleft lip subjects is compared to a group of normal subjects, and statistically significant differences have been found by univariate tests in the first approach. Further, our feature extraction method leads to an anatomically plausible set of landmarks for medical applications.

Keywords— asymmetry scores, cleft lip disfigurement, facial trauma surgery, feature selection, registration, shape analysis, size-and-shape, smile.

1 Introduction

Bilateral symmetry (left-right symmetry) is a key property in many biological settings. An object (treated as a set of unlabelled points known as landmarks) is said to be bilaterally symmetric if its reflection through some midline or midplane \mathcal{P} is exactly the same as the original object. In practice, exact bilateral symmetry seldom holds and it is of interest to study the extent of any asymmetry. Research about the symmetries of objects in the real world has a long history (see, for example, Weyl, 1952). Of particular interest is the hypothesis

of bilateral symmetry, especially in biology (Palmer and Strobeck, 1986). Statistical methods to test asymmetry were first formalized in Mardia et al. (2000). Subsequently, a wide variety of statistical methods have been developed; see, for examples, Kent and Mardia (2001), Bock and Bowman (2006), Ajmera et al. (2022) and Ajmera et al. (2023).

The focus of this paper is on landmark-based objects as in Mardia et al. (2000). Each object is a set of K labelled points or landmarks, represented as a $K \times M$ configuration matrix giving the positions of K landmarks in M dimensions. The cases $M = 2$ and $M = 3$ are the most important in practice. Call an object *bilateral* if its landmarks can be divided into two categories: *pairs* and *solos*, where paired landmarks locate on both sides of \mathcal{P} , while solos are unpaired. For a bilaterally symmetric object the two landmarks in a pair are equally spaced about the midplane and the solos lie on the midplane. If there are K_P pairs of landmarks and K_S solo landmarks, then the total number of landmarks is $K = 2K_P + K_S$. If the dataset has not been pre-registered, then registration is required. The details of registration are given in Section 2.1.

The asymmetry information in an object can be represented as a vector of *coordinatewise elementary asymmetry features*, \mathbf{d} , say, defined in more details in Section 2.2. Increasing the magnitude of any element of this vector indicates greater asymmetry. The elementary feature vector is also the starting point of Bock and Bowman (2006) and Patel et al. (2023) but we define its elements explicitly in Section 2.2.

Given two groups of objects, a natural question is whether one group is more asymmetric than the other. Section 3 looks at two testing strategies. In the first strategy the elements of the feature vector \mathbf{d} are combined into a single number called a *composite score*. Then a univariate test such as the two-sample t-test or the Mann-Whitney U test can be used to compare the two groups. The use of a univariate summary statistic for each object facilitates the comparison between objects and between groups of objects. The mathematical details are given in Section 3.1, our composite score extends the asymmetry measures used by Bock and Bowman (2006) and Patel et al. (2023).

In the second strategy, the two groups are compared using each of the elements in \mathbf{d} , yielding a collection of test statistics. The maximum of these test statistics gives an *overall test statistic* that can be used to test for a difference between the two groups. This approach is similar to the union-intersection test (UIT) in multivariate analysis, see, for example, Mardia et al. (2024). In particular, when the null hypothesis is rejected, it is possible to investigate which elementary features are responsible. The mathematical details are given in Section 3.2.

The motivation for the paper is given by a set of smile data on human subjects. Each subject was asked to smile, and a four-dimensional movie was made of the face (three spatial dimensions plus time using Di4D motion capture system). A set of landmarks was identified around the lips and followed through the frames of the movie. The subjects come from two groups: normal subjects and subjects who have had cleft lip surgery. The objective is to assess how successful the surgery has been; that is, are the cleft lip subjects any more asymmetric than normal people. The details of the smile data are provided in Section 4. The data is pre-registered and the objects at three fixed frames (the beginning, middle and end of the smile) are analyzed in Section 4 following Patel et al. (2023). We end the paper with some discussion in Section 5. The procedures for estimating the midline or midplane are given in

2 Describing asymmetry

2.1 Registration

We will introduce the following notations: let X , with elements $X[k, m]$, be a $K \times M$ configuration matrix giving the positions of K landmarks in M dimensions for a single object or subject or individual. We write as $X[k,] \in \mathbb{R}^M$ for the coordinates of k th landmark, $k = 1, \dots, K$. The most important choice for M is $M = 3$, and this case is emphasized in the presentation, but the mathematical theory is valid for any $M \geq 1$. In general, upper case letters are used for matrices and bold lower case letters for vectors. In addition the letters K, M, J are reserved for the number of landmarks, number of dimensions, and number of elementary features (Section 2.2), respectively, with typical indices given by the lower case letters k, m, j . In general, each data object X will be viewed as a noisy version of a bilaterally symmetric configuration.

Rigid body transformations If X is a configuration, then a *rigid body motion* takes X to $\mathbf{1}_M \mathbf{c}^T + XR = X^*$, say, where \mathbf{c} is an M -dimensional translation vector and R is an $M \times M$ rotation matrix. For the purposes of this paper, we say that X and X^* have the same *size-and-shape* following the standard terminology in shape analysis (see, for example, Dryden and Mardia (2016)). That is, the size-and-shape of X is the equivalence class of configurations under the group of rigid body motions. The asymmetry information carried by the size-and-shape is of interest and such information is unaffected under rigid body motion. The size is emphasized here, since the size information is taken into consideration. Recall that the term “shape” is a standard terminology in statistical shape analysis which means the equivalence class under the larger group of similarity transformations so the scale is also filtered out.

A hyperplane \mathcal{P} in \mathbb{R}^M can be written in the form $\mathcal{P} = \{\mathbf{x} \in \mathbb{R}^M : \mathbf{n}^T \mathbf{x} = b\}$, in terms of a unit normal vector \mathbf{n} , say, and a scalar offset term b , say. When $M = 3$ a hyperplane becomes a two-dimensional plane, and when $M = 2$ a hyperplane becomes a one-dimensional line. For simplicity we refer to hyperplanes as planes everywhere. Under a rigid body motion, \mathbf{n} is transformed to $R^T \mathbf{n}$ and b is transformed to $b + \mathbf{n}^T R \mathbf{c}$.

Two types of Registration For every bilateral data object X , suppose there is an associated midplane \mathcal{P} . Ways in which \mathcal{P} might be determined are discussed below. For data analysis, it is helpful to “register” X using a rigid body motion so that after transformation $\mathbf{n} = \mathbf{e}_1$ and $b = 0$, i.e., the midplane passes through the origin and the normal direction is given by the first coordinate axis, while still keeps the shape of X unchanged.

We will distinguish two types of registration:

1. Axis registration
2. Basis registration.

Axis registration takes the form described in the previous paragraph. In terms of the human

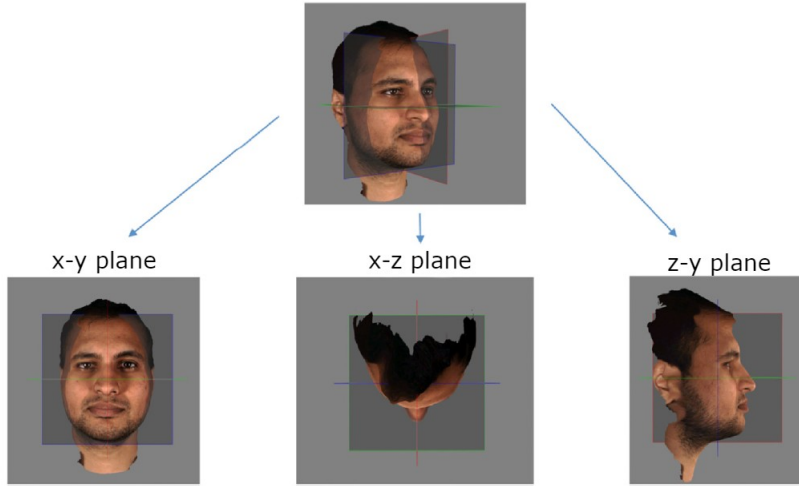


Figure 1: Coordinates system for human face with principal planes. (Source: Patel et al. (2023); coordinate labels have been corrected.)

head, after registration, the left-right axis lies along the first coordinate axis. However, the position of the down-up and back-front axes are not clearly distinguished from one another. It is possible to tilt the head forwards or backwards while still preserving axis registration.

In some settings it is possible to carry out a stronger version of registration, we will call *basis registration*, in which all the coordinate axes have a natural interpretation. For example, for 3D measurements of the human head, the midplane is known as the sagittal plane, and it is natural to require the coordinate axes to have the following interpretations:

- coordinate 1: left-right
- coordinate 2: down-up
- coordinate 3: back-front

Figure 1 shows these coordinate axes on a human face. Further details are given in Section 4.

To carry out axis registration it is necessary to know or estimate the midplane. There are three typical scenarios: (a) the midplane is known a priori; (b) the midplane has been estimated using expert knowledge, perhaps involving information beyond the landmarks themselves; or (c) the midplane is estimated from the landmark positions using Procrustes analysis. Scenario (c) is described in detail in Appendix A following Mardia et al. (2000) and Kent and Mardia (2001).

To carry out basis registration, it is also necessary to know or estimate the $M - 1$ remaining meaningful basis vectors in \mathcal{P} . In this case the three possibilities become: (a) the basis is known a priori; (b) the basis is estimated using expert knowledge, perhaps involving information beyond the landmarks themselves; or (c) hybrid Procrustes analysis. For details in Procrustes analysis, see, for example Dryden and Mardia (2016). By “hybrid”, we mean that (i) the normal direction to the midplane is estimated by combining an object with its reflection and using generalized Procrustes analysis (GPA), (ii) an “average shape” is found from all

the objects using GPA, (iii) the midplane for the average shape is oriented so the basis directions have natural interpretations using expert knowledge, and (iv) each data configuration is aligned to the average shape using ordinary Procrustes analysis. The details are given in Appendix A.

For the smile data application in Section 4, expert knowledge (scenario (b)) has been used to estimate the midplane with the stated interpretations for the coordinate axes as above in basis registration.

2.2 Elementary features

Suppose the size-and-shape dataset has been basis registered about a midplane \mathcal{P} that passes through the origin and is normal to the first coordinate axis. Then it is possible to define various elementary features to describe the asymmetry of each data object. Paired and solo landmarks are treated separately.

Let K_L and K_R denote the total number of landmarks on the left or right of \mathcal{P} . We have $K_L = K_R = K_P$. Let k_L and k_R denote the left and right indices for a typical landmark pair for a bilateral object X and consider the M *coordinatewise signed elementary features* for the landmark pairs,

$$d[(k_L, k_R), 1] = X[k_L, 1] + X[k_R, 1] \quad (2.1)$$

$$d[(k_L, k_R), m] = X[k_L, m] - X[k_R, m], \quad m = 2, \dots, M. \quad (2.2)$$

That is, there is one feature for each coordinate and each landmark pair. So there are in total MK_P coordinatewise features for all paired landmarks. For this specific \mathcal{P} , the first coordinates for the two landmarks in one pair have opposite signs, while other coordinates have the same sign. Further, for a symmetric object, the quantities in equations (2.1) and (2.2) should all be 0. Thus, taking the sum of the first coordinates and differences for other coordinates allow us to quantify the departure from symmetry. Similarly, if k_S is a typical solo landmark, consider the single elementary feature

$$d[(k_S)] = X[k_S, 1]. \quad (2.3)$$

There are in total K_S elementary features for solos. Under bilateral symmetry with \mathcal{P} chosen as above, the first coordinate of a solo landmark will be 0, with no restriction on other coordinates. Hence, a single feature as in (2.3) is adequate to describe the asymmetry of a solo landmark.

The coordinatewise elementary features can be collected into a *signed elementary feature vector* $\mathbf{d} = (d_j)$, say, of length $J_{\text{basis}} = MK_P + K_S$. The elements of \mathbf{d} will either be listed sequentially with a subscript index, i.e., d_j , $j = 1, \dots, J_{\text{basis}}$, or using parentheses within square brackets, as in (2.1)-(2.3).

When only axis registration is available, the coordinate information in (2.2) does not have a well-defined interpretation. This is because the coordinates except the first one of paired landmarks would be changed after rotation within \mathcal{P} , hence leads to changes in values of (2.2) even though the asymmetry information does not change. Note that the equation (2.1) will

not change. Further, at each landmark the coordinate information can be collected into a single number, called a *landmark elementary feature* which is defined per landmark,

$$d^*[(k_L, k_R)] = \left\{ \sum_{m=1}^M d^2[(k_L, k_R), m] \right\}^{1/2}, \quad (2.4)$$

which does have a well-defined interpretation as the Euclidean distance between one landmark in a pair and the reflection of the other landmark in the pair. Rotation within \mathcal{P} would not change this Euclidean distance. For a solo landmark, (2.3) is always well defined since the first coordinate of a solo remains unchanged after rotation within \mathcal{P} ; hence it is both a coordinatewise and a landmark elementary feature. Thus, overall in the case of axis registration, a smaller set of $J_{\text{axis}} = K_P + K_S$ elementary features can be collected into a vector for further analysis. On the other hand, for $M = 2$, there is no difference between axis and basis registration. Thus, equations (2.1)-(2.3) are all valid for both types of registrations in this case.

Another useful way to think about the elementary features is by using reflection. Let X be a basis registered configuration, and let $X^{(\text{refl})}$ denote the reflection of X about \mathcal{P} . Computationally, this matrix is obtained by changing the sign of the first column of X and interchanging the row indices for each landmark pair. Then the elementary features of X can be obtained by comparing the elements of X and $X^{(\text{refl})}$. If X is bilaterally symmetric about \mathcal{P} , then $X = X^{(\text{refl})}$ and elementary features vanish, i.e. $\mathbf{d} = \mathbf{0}$.

In many examples, such as the smile application studied later in this paper in Section 4, the direction of asymmetry, for example, left or right asymmetry, can vary between individuals and is not thought to be interested. We will focus on the absolute values of the elementary features. Define the *absolute elementary feature vector* \mathbf{a} with elements

$$a_j = |d_j|, \quad j = 1, \dots, J, \quad (2.5)$$

where $J = J_{\text{basis}}$ or $J = J_{\text{axis}}$, as appropriate. In other words, only the extent of the asymmetry is interested. The elements of \mathbf{a} can also be written in a similar way as elements of \mathbf{d} in (2.1)-(2.3). In the rest of the paper, each configuration X is reduced to an absolute elementary feature vector \mathbf{a} for further numerical and statistical analysis.

2.3 A Simple Illustrative Example

To illustrate the construction of the vector \mathbf{a} , consider two configurations in $M = 2$ dimensions with $K = 4$ landmarks given by

$$X_1 = \begin{pmatrix} -1 & 0 \\ 0 & 1 \\ 1 & 0 \\ 0 & -1 \end{pmatrix}, \quad X_2 = \begin{pmatrix} -0.95 & 0.36 \\ -0.28 & 2.11 \\ 0.99 & 0.54 \\ -0.31 & -1.37 \end{pmatrix}. \quad (2.6)$$

Suppose the landmarks consist of one landmark pair, $(k_L, k_R) = (1, 3)$ and two solos, $k_S = 2, 4$. Hence $K_P = 1$ and $K_S = 2$. Further, suppose both configurations are treated as basis registered with \mathcal{P} normal to the first coordinate axis, i.e. \mathcal{P} is the y -axis.

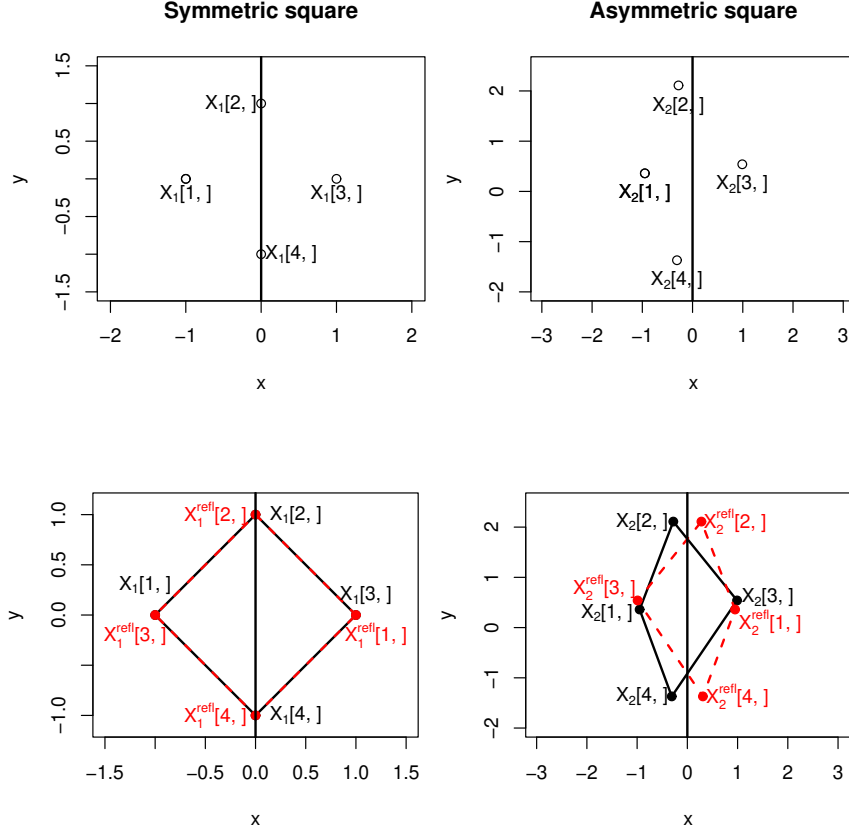


Figure 2: The left and right figures in the top row show the original configurations of symmetric square X_1 and asymmetric square X_2 (in black) respectively. The left and right figures in the bottom row show the original objects (in black solid lines) together with their respective reflections $X_1^{(refl)}$ and $X_2^{(refl)}$ (in red dotted lines) respectively, in order to illustrate the coordinatewise elementary feature vector.

The configurations X_1 and X_2 are shown in the left and right figures in the top row of Figure 2 respectively, whereas the bottom row of Figure 2 show their corresponding reflections, where the left is for X_1 and $X_1^{(refl)}$ and right is for X_2 and $X_2^{(refl)}$. Note that X_1 is bilaterally symmetric, with $\mathbf{a} = \mathbf{0}$. Table 1 gives the $J_{basis} = 4$ elements of the vector \mathbf{a} for X_2 . The two elements for the landmark pair are listed first, and the two elements for the solos listed last, with $\mathbf{a} = (0.04, 0.18, 0.28, 0.31)^T$ for X_2 . It can be seen visually in Figure 2 that for X_2 , landmarks 2 and 4 deviate more from the y -axis than the landmark pair (1, 3) differs from symmetry. Hence the last two components of \mathbf{a} are larger than the first two components.

3 Hypothesis tests

Consider a dataset of N basis registered configurations observed on two groups of individuals, where the first N_1 configurations belong to one group and the last N_2 configurations belong to the other group, $N = N_1 + N_2$, where it is thought that the first group of configurations might

Table 1: Example in Section 2.3. Elements of the absolute elementary feature vector $\mathbf{a} \in \mathbb{R}^4$ for X_2 with $K = 4$ landmarks in $M = 2$ dimensions.

Landmark Indices	Coordinate Axis	Feature of \mathbf{a}	value of \mathbf{a}
Pair (1,3)	1	$a[(1, 3), 1] = X_2[1, 1] + X_2[3, 1] $	0.04
Pair (1,3)	2	$a[(1, 3), 2] = X_2[1, 2] - X_2[3, 2] $	0.18
Solo 2	1	$a[(2)] = X_2[2, 1] $	0.28
Solo 4	1	$a[(4)] = X_2[4, 1] $	0.31

be less asymmetric than the second. One way to think about this question is to construct a one-sided hypothesis test of

$$\begin{aligned} H_0 &: \text{the two groups have the same distribution of asymmetry vs.} \\ H_1 &: \text{Group 1 is less asymmetric than Group 2.} \end{aligned} \quad (3.1)$$

We will give two general approaches to construct a test statistic: (a) combine-then-compare, and (b) compare-then-combine. These two approaches will be explored in the next subsections.

To specify the null and alternative hypotheses explicitly, some notations are needed. Suppose the data take the form of N registered configurations

$$X_n, \quad n = 1, \dots, N. \quad (3.2)$$

Let \mathbf{a}_n denote the corresponding absolute elementary feature vector for X_n (equation (2.5)), with elements a_{nj} , $j = 1, \dots, J$ and $J = J_{\text{basis}}$ for the rest of this paper.

Then the hypotheses given in equation (3.1) can be reformulated as:

$$\begin{aligned} H_0 &: \mathbf{a}_n \sim F \text{ i.i.d. for all } n \text{ vs.} \\ H_1 &: \mathbf{a}_n \sim F_1 \text{ i.i.d. for } n = 1, \dots, N_1, \mathbf{a}_n \sim F_2 \text{ i.i.d. for } n = N_1 + 1, \dots, N, \end{aligned} \quad (3.3)$$

where F , F_1 , F_2 are multivariate cumulative density functions (c.d.f.s) and F_1 is stochastically smaller than F_2 (that is, $F_1(\mathbf{a}) \geq F_2(\mathbf{a})$ for all \mathbf{a} with at least one strict inequality), see, for example Stoyan (1983). In other words, the distribution of F_2 is shifted towards right comparing with F_1 , which indicates more asymmetries.

We concentrate in this section on t-test and Mann-Whitney U test. In Section 4, we further discuss some alternative univariate tests as well as multivariate tests in relation to the smile data.

3.1 Testing strategy: combine-then-compare

Each element a_j of \mathbf{a} (equation (2.5)) is nonnegative and a larger value of a_j indicates greater asymmetry. Hence it is natural to reduce the J -dimensional vector \mathbf{a} to a single number by combining the elements of \mathbf{a} into a *composite asymmetry score*

$$u = \phi(\mathbf{a}), \quad (3.4)$$

say. Here the function $\phi(\mathbf{a})$ is assumed to be monotonically increasing in the sense that it is monotonically increasing in each component a_j when the other elements are held fixed.

Let $\psi(a)$ be a monotonically nonnegative increasing function of a scalar argument $a \geq 0$. Then one way to define $\phi(\mathbf{a})$ is as an *additive composite asymmetry score*

$$\phi_{\psi, \mathbf{w}}(\mathbf{a}) = \sum_{j=1}^J w_j \psi(a_j), \quad (3.5)$$

where the $w_j \geq 0$ are pre-assigned weights. Some choices for weights include the following:

- (a) equal weights $w_j = 1$,
- (b) greater weights near the midplane,
- (c) greater weights away from the midline, or
- (d) different weights for pairs and solos.

For example, in cases (b) and (c) a weight might depend on $|X[k_R, 1] - X[k_L, 1]|$ for a landmark pair, with solos treated separately. The choices of weights in general depend on prior belief of the extent of asymmetry information carried by each landmark, for example, if it is known a priori that landmarks far away from \mathcal{P} can carry important asymmetry information than landmarks near \mathcal{P} , then more weights should be assigned to the farther landmarks. For smile example, this information is available so greater weights will be given near the midplane, see Section 4.

The choice of function ψ governs the relative influence of different magnitudes of an elementary feature. For example, the quadratic function $\psi(a) = a^2$ is more sensitive to outlying features than the linear function $\psi(a) = a$.

We write below explicitly for two such scores with equal weights and give them names L_1 and L_2 statistics respectively.

$$L_1 \text{ statistic: } \phi_{L_1}(\mathbf{a}) = \sum_{j=1}^J a_j = \sum_{(k_L, k_R)} \sum_{m=1}^M |d[(k_L, k_R), m]| + \sum_{k_S} |d[(k_S)]|, \quad (3.6)$$

$$L_2 \text{ statistic: } \phi_{L_2}(\mathbf{a}) = \sum_{j=1}^J a_j^2 = \sum_{(k_L, k_R)} \sum_{m=1}^M d[(k_L, k_R), m]^2 + \sum_{k_S} d[(k_S)]^2. \quad (3.7)$$

In the above equations, we use the two expressions for elements in \mathbf{d} and \mathbf{a} introduced in Section 2.2.

Bock and Bowman (2006) have proposed an asymmetry score with weights $w_j = 1$ for landmark pairs and weights $w_j = 2$ for solos and $\psi(a_j) = a_j^2$ in equation (3.5), namely,

$$\sum_{(k_L, k_R)} \sum_{m=1}^M d[(k_L, k_R), m]^2 + 2 \sum_{k_S} d[(k_S)]^2. \quad (3.8)$$

	$d^*[(1, 3)]$ (2.4)	$\phi_{L_1}(\mathbf{a})$ (3.6)	$\phi_{L_1}^*(\mathbf{a})$ (3.9)	$\phi_{L_2}(\mathbf{a})$ (3.7)
X_2	0.18	0.81	0.39	0.21

Table 2: The two composite asymmetry scores defined in equation (3.5) and equation (3.9) are computed on the configuration X_2 .

For our work, we have selected an equal weights for ϕ_{L_1} to have some similarity to the asymmetry score of Patel et al. (2023); their score is given by

$$\phi_{L_1}^*(\mathbf{a}) = \sum_{(k_L, k_R)} d^*[(k_L, k_R)] + \sum_{k_S} |d[(k_S)]|, \quad (3.9)$$

with weights equal to 1 for both pairs and solos. The $d^*[(k_L, k_R)]$ is defined in equation (2.4). Also, we can define a similar score as follows using L_2 distances

$$\phi_{L_2}^*(\mathbf{a}) = \sum_{(k_L, k_R)} d^*[(k_L, k_R)]^2 + \sum_{k_S} |d[(k_S)]|^2. \quad (3.10)$$

It can be shown using (2.4) that this equation (3.10) reduces to (3.7). That is, we have

$$\phi_{L_2}^*(\mathbf{a}) = \phi_{L_2}(\mathbf{a}).$$

Note that, we can generalize $\phi^*(\mathbf{a})$ in the same way as $\phi(\mathbf{a})$ with weights.

Example in Section 2.3 continued. Recall the asymmetric square X_2 defined in equation (2.6). The configuration is shown in Figure 2. The landmark elementary feature, $d^*[(1, 3)]$, defined in equation (2.4) is computed and reported in Table 2. The composite asymmetry scores $\phi_{L_1}(\mathbf{a})$ (3.6), scaled $\phi_{L_1}^*(\mathbf{a})$ (3.9) (divided by the number of landmarks) and $\phi_{L_2}(\mathbf{a})$ (3.7) are computed on X_2 for illustration. The results are shown in Table 2. Note that the values of

$$d^*[(1, 3)] = \sqrt{(X_2[1, 1] + X_2[3, 1])^2 + (X_2[1, 2] - X_2[3, 2])^2} = 0.18$$

and $a[(2)] = 0.28$, $a[(4)] = 0.31$ (Table 1) are less than 1, so taking squares of them in ϕ_{L_2} leads to smaller values. Note that here we have scaled $\phi_{L_1}^*$ by a factor of half, so unscaled $\phi_{L_1}^* = 0.78$ which is similar to the value of $\phi_{L_1} = 0.81$.

Once a composite asymmetry score $\phi(\mathbf{a})$ has been chosen, let

$$u_n = \phi(\mathbf{a}_n), \quad n = 1, \dots, N, \quad (3.11)$$

denote the composite asymmetry scores for the data in (3.2).

Let

$$\mu_g = E\{U_g\}, \quad \sigma_g^2 = \text{var}\{U_g\} \quad (3.12)$$

denote the expectation and variance for a random variable $U_g \sim F_g$, where $g = 1, 2$ labels one of the two groups. A simpler version of hypotheses in (3.1) is

$$H_0 : \mu_1 = \mu_2 \text{ vs. } H_1 : \mu_1 < \mu_2 \quad (3.13)$$

There are several test statistics that can be used for testing hypotheses given in (3.1) and (3.13), including the following:

- (a) the standard two-sample t-test, which assumes a common variance for the two groups ($\sigma_1^2 = \sigma_2^2$);
- (b) the Mann-Whitney U test, also known as the Wilcoxon rank sum test (Mann and Whitney, 1947).

The Mann-Whitney U test is nonparametric so that the test results are invariant under monotonic transformations of the u_n . In case (a), the significance of the test statistic under H_0 can be computed either analytically (assuming normality) or using a bootstrap approximation. In case (b) the significance can be derived from combinatorial arguments. Mann-Whitney U test is considered where the normality assumption on composite asymmetry scores $u_n = \phi(\mathbf{a}_n)$ may fail to hold.

An advantage of the combine-then-compare approach is that it enables us to accumulate evidence from different features. If there is a small amount of asymmetry on many different elementary features, then the composite score will have a large value. Further, this approach enables the two groups to be compared visually with stem and leaf plots and in particular, any overlap between the two groups can be easily assessed. Applications of this approach are in Section 4

3.2 Testing strategy: compare-then-combine

In this approach, separate test statistics are constructed for each feature in the elementary feature vectors. The most extreme of these separate test statistics is then used as an overall test statistic. Before we give the details, the hypotheses in equation (3.1) need to be formulated in the union intersection test style (as explained in Section 1) as following:

$$H_0 = \bigcap_{j=1}^J H_0^j \text{ vs } H_1 = \bigcup_{j=1}^J H_1^j, \quad (3.14)$$

where H_0^j : the mean of j th unsigned elementary feature between the two groups is the same, whereas H_1^j is that the mean of group 2 is larger than mean of group 1, for $j = 1, \dots, J$.

For each choice j of an unsigned elementary feature, construct a statistic to compare the two groups, for example, a two-sample t-statistic or a Mann-Whitney U statistic. Denote the resulting statistics by v_j , $j = 1, \dots, J$. For example, if a t-statistic is used, then

$$v_j = (\bar{a}_j^{(1)} - \bar{a}_j^{(2)})/s_j. \quad (3.15)$$

where $\bar{a}_j^{(g)}$, $g = 1, 2$ are the sample means of the j th unsigned elementary feature in the two groups and s_j^2 is the pooled within-group variance.

An overall UIT statistic to test H_0 vs H_1 in equation (3.14) can be defined by taking the maximum of these separate statistics (Boyett and Shuster, 1977),

$$V = \max_{j=1, \dots, J} v_j. \quad (3.16)$$

The critical points of V under the null hypothesis can be computed by the bootstrap. Note that the landmarks are correlated with each other, so the d_j are not independent for $j = 1, \dots, J$ here, so we cannot derive the distribution of V theoretically. Hence, bootstrap is used for estimating the critical points of V .

If there exists v_j which exceeds the critical values of V , then we not only know that H_0 is rejected, but also know that the landmark corresponding to such v_j is also important.

Our main aim is somewhat different from Boyett and Shuster (1977): we aim at selecting important landmarks while Boyett and Shuster (1977), attempt to estimate a p -value. The bootstrap procedure used by us is also different from their who have used:

1. A set E containing all permutations of the dataset is constructed.
2. Sample with replacement from this set E , i.e. sample permutations of the data. The permuted samples constitute the bootstrap resampled dataset.
3. Test statistic V is computed on the resampled dataset.

On the other hand, we directly sample from the whole dataset as following:

1. Sample N samples with replacement from $\{\mathbf{a}_n\}_{n=1}^N$.
2. Compute v_j and V on resampled dataset.

An advantage of this compare-then-combine approach versus combine-and-compare is that if the null hypothesis is rejected, then simultaneous confidence intervals can be constructed to identify those features on which the two groups significantly differ. The selection procedure in spirit is similar to Tukey’s method (Tukey, 1949) in ANOVA though in ANOVA a separate test statistic is used for each pairwise difference between main effects. Here, a separate test statistic for each j is more appropriate since all features in unsigned elementary feature vector \mathbf{a} have different biology. An illustration is given below for the smile data.

4 Analyses of the Smile Data

We now give smile data taken from Patel et al. (2023) which have been pre-registered. The data is collected using the Di4D system. When a subject’s face is placed in front of the camera, the x -axis is positioned horizontally on the face (positive direction is left), the y -axis is placed vertically on the face (positive direction is upward), whereas the z -axis is positioned in the direction inwards and outwards of the face (positive direction is outward), see Figure 1.

The coordinates given in Section 2.1 can be related to these coordinate axes as follows:

- coordinate 1: left-right x
- coordinate 2: down-up y
- coordinate 3: back-front z .

Our smile data contains $N = 25$ subjects, of which $N_1 = 12$ are control subjects and $N_2 = 13$ are cleft subjects. There are $K = 24$ landmarks on the lip periphery. Figure 3 shows the lip

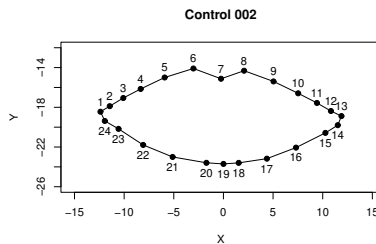


Figure 3: Landmark indices for x - y coordinates on the lip periphery of a control subject at first frame.

Table 3: Indices of landmark pairs and solos in Figure 3 on the lip periphery.

Landmark notation	Indices in Figure 3
pair (k_L, k_R)	(1,13), (2,12), (3, 11), (4,10), (5,9), (6,8), (20,18), (21,17), (22,16), (23,15), (24,14)
k_S	7, 19

Table 4: Mean, variance, t-values and p -values for $\phi_{L_1}^*(\mathbf{a})$ (equation (3.9)) for cleft and control subjects at first, middle and last frames (Patel et al. (2023)).

	Cleft		Control		One-sided test	
	mean	sd	mean	sd	t -values	p -values
First	1.78	0.46	1.12	0.41	3.86	0.0004(***)
Middle	1.96	0.70	1.46	0.47	2.14	0.02(*)
Last	2.14	0.80	1.55	0.43	2.34	0.01(**)

(*) = significant at the 5% significance level. (**) = significant at the 1% significance level. (***) = significant at the 0.1% significance level.

configuration in the x - y plane. There are $K_P = 11$ landmark pairs and $K_S = 2$ solo landmarks. The landmark indices are summarized in Table 3. The $M = 3$ dimensional coordinates of these landmarks have been extracted at three frames: first (closed lip), middle (middle of the smile) and last frame (maximum open lip smile). Let $g = 1, 2$ denote the control and cleft groups, respectively.

In the rest of this section several test statistics will be presented in two parts; combine-then-compare approach and compare-then-combine approach.

Combine-then-compare approach using (3.9). Patel et al. (2023) carried out standard two-sided two-sample t-tests using the statistic (3.9), with conventional t-tables used to judge significance. Here we report the results of the one-sided versions of these t-tests since based on hypotheses in (3.1), one-sided tests are more appropriate. The results of our t-tests are given in Table 4. We reach the same conclusions as in Patel et al. (2023) for their two-sided tests, namely, H_0 is rejected at all three frames. Further, the one-sided t-test indicates that there is more asymmetry for cleft lip subjects versus controls. Note that here the p -value is the smallest at the first frame, which suggests that the two groups are the most different at the start.

Table 5: p -values from one-sided two-sample Mann-Whitney U tests using $\phi_{L_1}(\mathbf{a})$ (3.6) and $\phi_{L_2}(\mathbf{a})$ (3.7).

Composite asymmetry score	First frame	Middle frame	Last frame
$\phi_{L_1}(\mathbf{a})$	$9.69 \times 10^{-5}(\text{***})$	0.026(*)	0.009(**)
$\phi_{L_2}(\mathbf{a})$	0.0002(***)	0.011(*)	0.013(*)
weighted $\phi_{L_1}(\mathbf{a})$	0.002(**)	0.008(**)	0.002(**)
weighted $\phi_{L_2}(\mathbf{a})$	0.013(*)	0.015(*)	0.005(**)

(*) = significant at the 5% significance level. (**) = significant at the 1% significance level. (***) = significant at the 0.1% significance level.

Combine-then-compare approach using (3.6) and (3.7). We use the scores $\phi_{L_1}(\mathbf{a})$ and $\phi_{L_2}(\mathbf{a})$ defined in equations (3.6) and (3.7) respectively. Instead of considering asymmetries with respect to each landmark as in (3.9), we view all features in \mathbf{a} as a whole and take the L_1 and L_2 norms. For the subjects which are more symmetric, their corresponding \mathbf{a}_n should be close to the origin. Hence, the L_1 and L_2 distances between \mathbf{a}_n with $\mathbf{0} \in \mathbb{R}^J$ should be smaller for control subjects. Several one-sided two-sample Mann-Whitney U tests have been performed and the results are shown in Table 5. For the last two rows in the table, the weighted $\phi_{L_1}(\mathbf{a})$ and weighted $\phi_{L_2}(\mathbf{a})$ are used and w_j are chosen in an adaptive way as the following:

1. Compute the sample mean shape on the augmented data, which contains basis registered original configurations and their reflections through midplane. Since the data has been pre-registered, the sample mean shape is simply the arithmetic mean for each landmark.
2. The Euclidean distance within each landmark pair for this mean shape is computed and its reciprocal is used as the weight. The weights are the same among these subjects from both groups. The weights for solo landmarks are the unit length based on the scale of data.

Different landmarks carry different amount of asymmetry information. Those landmarks near the midplane \mathcal{P} may carry the most significant information on asymmetry according to the expert's knowledge. Thus, we give higher weights to landmarks near \mathcal{P} and smaller weights on landmarks faraway from the central.

It can be seen from Table that 5 H_0 is rejected in all cases. In summary, there are significant differences between cleft and control subjects at all frames, with control subjects less asymmetric than cleft subjects overall.

Since the test results indicate significant differences between the two groups, we would like to visualize the separation between the distributions of composite asymmetry scores of the two groups. Hence, dot plots similar to the stem leaf plot are created and given in Figures 4, 5, 6, 7 and 8. In these dot plots, composite asymmetry scores for both groups are plotted together at each frame.

Figure 4 shows the dot plots for $\phi_{L_1}^*(\mathbf{a})$ defined in equation (3.9), whereas Figure 5 and 6 display the dot plots of $\phi_{L_1}(\mathbf{a})$ and $\phi_{L_2}(\mathbf{a})$ (equations (3.6) and (3.7)) respectively. According to

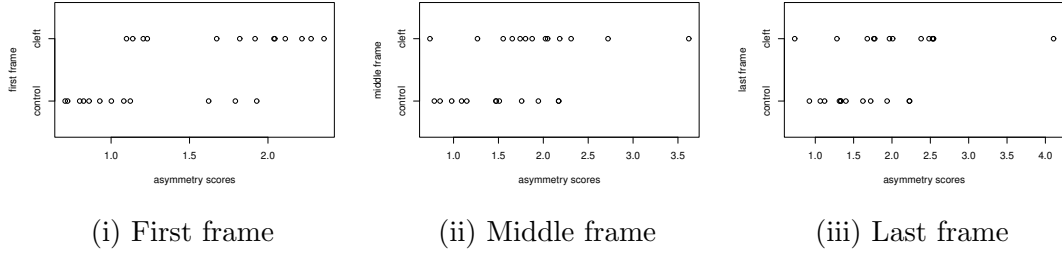


Figure 4: Dot plots of $\phi_{L_1}^*(\mathbf{a})$ defined in equation (3.9) at the three frames. The top row of the graph is for cleft lip subjects whereas the bottom row is for controls.

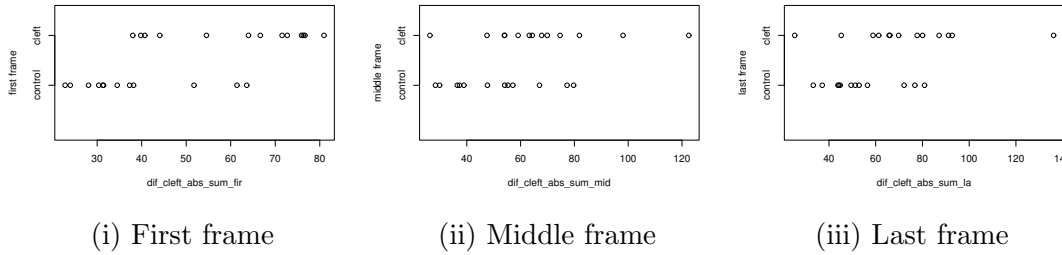


Figure 5: Dot plots of $\phi_{L_1}(\mathbf{a})$ (3.6) at the three frames. The top row of the graph is for cleft lip subjects whereas the bottom row is for control subjects.

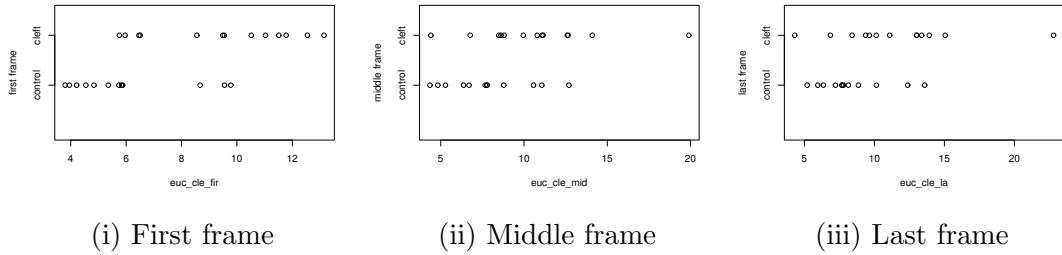


Figure 6: Dot plots of $\phi_{L_2}(\mathbf{a})$ (3.7) at the three frames. The top row of the graph is for cleft lip subjects whereas the bottom row is for control subjects.

these dot plots, substantial overlaps between cleft and control subjects can be seen. Moreover, the three composite asymmetry scores used in this section all have similar performances, as the separation between the two groups at each frame revealed by the dot plots are all similar.

Figure 7 and 8 show the dot plots for weighted $\phi_{L_1}(\mathbf{a})$ and weighted $\phi_{L_2}(\mathbf{a})$ respectively. According to these figures, these two composite scores push outliers farther away, i.e., they are sensitive to outliers, especially for weighted $\phi_{L_2}(\mathbf{a})$. So the weighted $\phi_{L_1}(\mathbf{a})$ and weighted $\phi_{L_2}(\mathbf{a})$ emphasize which are more extreme in cleft lip group.

Compare-then-combine approach using (3.4). The method described in Section 3.2 is used to select the landmarks which possess significant asymmetry information. v_j is selected to be the two-sample t-statistics (equation (3.15)). V defined in (3.16) is computed and its critical value at 5% significance level is determined via bootstrap. The total number of

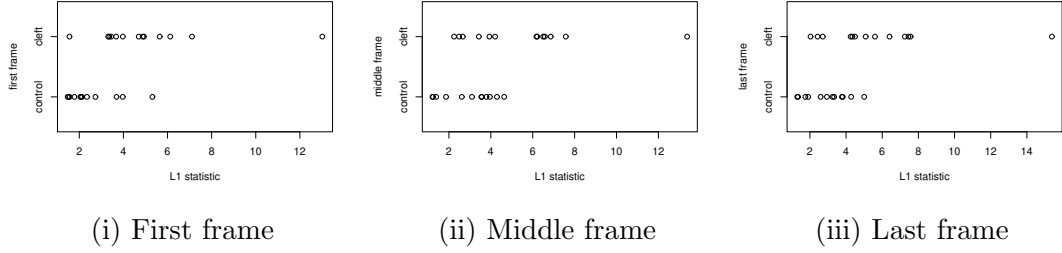


Figure 7: Dot plots of weighted $\phi_{L_1}(\mathbf{a})$ at the three frames. The top row of the graph is for cleft lip subjects whereas the bottom row is for control subjects.

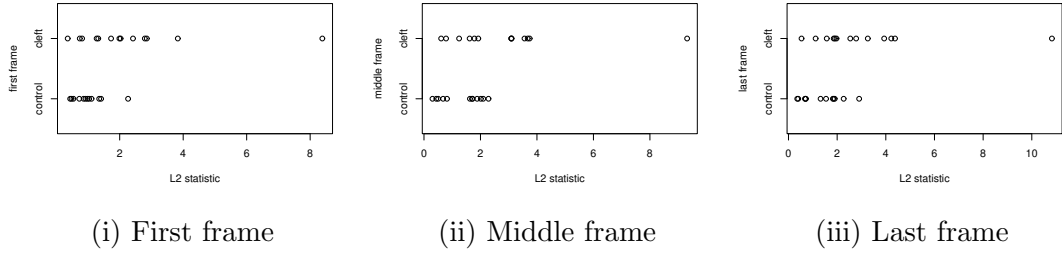


Figure 8: Dot plots of weighted $\phi_{L_2}(\mathbf{a})$ at the three frames. The top row of the graph is for cleft lip subjects whereas the bottom row is for control subjects.

bootstrap iterations used was 10000. Boyett and Shuster (1977) suggest 17000 iterations to make sure the significance level is 1%. However, the results of using 10000 and 17000 iterations turned out to be the same for our smile data. The central pair, landmarks 6 and 8, correspond to t -values which exceed these critical points at all three frames. Thus, these two landmarks have the most significant information of asymmetry. Further, the simultaneous confidence interval related to landmarks 6 and 8 excludes 0, so that H_0 is rejected when use these landmarks.

Further, most of the extreme p -values are obtained from Mann-Whitney U tests related to landmarks 6, 8 and two solo landmarks 7 and 19. These tests are performed using ϕ_{L_1} and ϕ_{L_2} computed on various subsets of landmarks. This suggests that the two groups are differed at most when using these four landmarks. So these landmarks can carry important information on asymmetries. This finding matches the expert's opinion. Figure 9 shows a photo of a cleft patient, where the central pair (6, 8) and solo landmarks, 7 and 19, are marked on the photo and the landmarks are same as in Figure 3. Roughly, it is a 'Y'-shape if we join the landmarks 6, 7, 8 and then 7 with 19 by line segments. From medical point of view, this particular shape is known a priori to be the most important for the asymmetry assessment.

We also applied the Welch version of the t -test (Welch, 1947), which accommodates different variances for the two groups. In this example, the results of the Welch t -test is found to be similar to the standard t -test (Table 4). A possible reason is that our sample size is small, so it results into similar outcome. Further, the multivariate Hotelling's T^2 test on unsigned elementary feature vector \mathbf{a}_n , $n = 1, \dots, N$, is an alternative approach to the UIT. In this example, the test results fail to improve the outcomes of the univariate tests. It could be

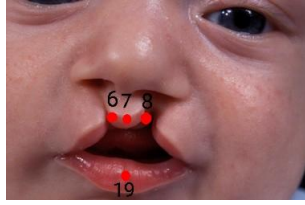


Figure 9: Photo of a cleft patient with central pair landmarks and solo landmarks. This figure is reproduced from photo taken from the website <https://www.nhs.uk/conditions/cleft-lip-and-palate/>.

since a Hotelling's T^2 test treats the features separately so it does not gain any power if the features point in the same direction; one-sided Hotelling's T^2 could be appropriate approach, which we will pursue in future. In this example, the sample size is less than the dimension of \mathbf{a}_n , i.e. $N < J$, so the covariance matrix is singular, which requires some modifications and will be dealt in future.

We end this section by summarizing the main conclusions for this smile data:

- There are statistically significant differences between the two groups at all frames. So overall, control subjects are less asymmetric than the cleft lip subjects.
- Substantial overlaps can be found on dot plots in Figure 4, 5 and 6. This matches the expert's expectation that some cleft lip subjects should be fairly close to normal subjects after surgeries.
- The landmarks 6, 7, 8 and 19 (the 'Y'-shape) are the most important in assessing asymmetries.

5 Discussion

We have presented our work for pre-registered data, but it can be extended when the landmark data is not pre-registered as pointed out in Section 4. Further, these revised measures of asymmetry can be applied and analyzed in a straightforward way. Further, we have used only size-and-shape framework but it can be extended easily to include for example, similarity shape.

We have used absolute values (a_j) on coordinate elementary features as in equation (2.5) which is of main interest if one is looking for the extent of asymmetry as in our case for the smile data. However, there maybe some other applications where raw d_j may be important than a_j ; our work easily applies to that situation.

In this paper we have concentrated on smile example with three fixed frames. Our future statistical work will be extended to dynamic shape analysis which will allow to study trajectories of the smile. Some initial work for a single group of a smile data has been introduced in Mardia et al. (2018) and Bookstein et al. (2024). We have concentrated on the cleft lip subjects but there are other medical applications such as in facial reconstruction related to trauma surgery where the lips form significant area for surgery.

We have used univariate methods but we can use Hotelling's T^2 in place of t-statistics, for example, though it requires some modifications. An one-sided alternative seems natural according to equation (3.1) and in future we would consider one-sided multivariate tests. Nevertheless, it requires more care to set up than in the one-dimensional case. Further, the scenario of sample size is less than the dimension of the data vector has also to be taken into account.

Acknowledgements

The authors would like to thank the School of Mathematics, University of Leeds for supporting the smile project. Kanti Mardia acknowledges the Leverhulme Trust for the Emeritus Fellowship.

Appendix A Estimation of midplane using Procrustes analysis

Let $\mathbf{n} \in \mathbb{R}^M$ denote the unit normal vector of an arbitrary plane \mathcal{P}' . Let $X_n \in \mathbb{R}^{K \times M}$, $n = 1, \dots, N$ denote the observed configurations. The reflection of X_n about \mathcal{P}' , $X_n^{(\text{refl})}$, is given as

$$X_n^{(\text{refl})} = X_n H,$$

where $H = I_M - 2\mathbf{n}\mathbf{n}^T$ is the Householder matrix and I_M is the $M \times M$ identity matrix. Then the estimation process used in basis registration is given as the following:

1. Form an augmented dataset: $\{X_n, X_n^{(\text{refl})}\}_{n=1}^N$.
2. Apply GPA on this augmented dataset. Denote the fitted configurations as $X_n^{(\text{GPA})}$ for $n = 1, \dots, N$.
3. Compute the Procrustes mean shape. This mean shape will be bilaterally symmetric with midplane \mathcal{P}' .
4. Rotate the mean shape outside and within \mathcal{P}' until the new midplane and the basis are meaningful.
5. Carry out ordinary Procrustes analysis between each $X_n^{(\text{GPA})}$ and the rotated mean shape.

When axis registration is considered, we only rotate the sample mean shape outside midplane. Further, the last step, step 5, is ignored. Further details are given for this procedure in Mardia et al. (2000).

References

- Ajmera, D. H., Hsung, R. T., Singh, P., Wong, N. S. M., Yeung, A. W. K., Lam, W. Y. H., Khambay, B. S., Leung, Y. Y. and Gu, M. (2022) Three-dimensional assessment of facial asymmetry in class III subjects. Part 1: a retrospective study evaluating postsurgical outcomes. *Clin Oral Invest*, **26**, 4947–4966.
- Ajmera, D. H., Zhang, C., Ng, J. H. H., Hsung, R. T., Lam, W. Y. H., Wang, W., Leung, Y. Y., Khambay, B. S. and Gu, M. (2023) Three-dimensional assessment of facial asymmetry in class III subjects, part 2: evaluating asymmetry index and asymmetry scores. *Clin Oral Invest*, **27**, 5813–5826.
- Bock, M. T. and Bowman, A. W. (2006) On the measurement and analysis of asymmetry with applications to facial modelling. *Journal of the Royal Statistical Society: Series C (Applied Statistics)*, **55**, 77–91.
- Bookstein, F. L., Kent, J. T., Khambay, B. S. and Mardia, K. V. (2024) Bridging geometric morphometrics to medical anatomy: An example from an experimental study of the human smile. *bioRxiv*. URL: <https://www.biorxiv.org/content/10.1101/2024.03.07.583999v1>.
- Boyett, J. M. and Shuster, J. J. (1977) Nonparametric one-sided tests in multivariate analysis with medical applications. *Journal of the American Statistical Association*, **72**, 665–668.
- Dryden, I. L. and Mardia, K. V. (2016) *Statistical Shape Analysis: With Applications in R*. Wiley.
- Kent, J. T. and Mardia, K. V. (2001) Shape, Procrustes tangent projections and bilateral symmetry. *Biometrika*, **88**, 469–485.
- Mann, H. B. and Whitney, D. R. (1947) On a test of whether one of two random variables is stochastically larger than the other. *The Annals of Mathematical Statistics*, **18**, 50–60.
- Mardia, K. V., Bookstein, F. L., Khambay, B. S. and Kent, J. T. (2018) Deformations and smile: 100 years of D’Arcy Thompson’s On Growth and Form. *Significance*, **15**, 20–25.
- Mardia, K. V., Bookstein, F. L. and Moreton, I. J. (2000) Statistical assessment of bilateral symmetry of shapes. *Biometrika*, **87**, 285–300.
- Mardia, K. V., Kent, J. T. and Taylor, C. C. (2024) *Multivariate Analysis, Second Edition*. Wiley.
- Palmer, A. R. and Strobeck, C. (1986) Fluctuating asymmetry: Measurement, analysis, patterns. *Annual Review of Ecology and Systematics*, **17**, 391–421.
- Patel, Y., Sharp, I., Enocson, L. and Khambay, B. S. (2023) An innovative analysis of nasolabial dynamics of surgically managed adult patients with unilateral cleft lip and palate using 3D facial motion capture. *Journal of plastic, reconstructive and aesthetic surgery*, **85**, 287–298.
- Stoyan, D. (1983) *Comparison Methods for Queues and Other Stochastic Models*. Wiley.

- Tukey, J. W. (1949) Comparing individual means in the analysis of variance. *Biometrics*, **5**, 99–114.
- Welch, B. L. (1947) The generalization of “Student’s” problem when several different population variances are involved. *Biometrika*, **34**, 28–35.
- Weyl, H. (1952) *Symmetry*. Princeton University Press.